EA Thermally - Induced Fractures in Coal, Balingian Province, Sarawak, Malaysia*

Yasir Ali Ibrahim[1] and Eswaran Padmanabhan[2]

Search and Discovery Article #80674 (2019)**
Posted March 11, 2019

*Adapted from extended abstract prepared in conjunction with oral presentation given at 2018 International Conference and Exhibition, Cape Town, South Africa, November 4-7, 2018
 DOI:10.1306/80674Ibrahim2019

[1]Red Sea University, Port Sudan, Sudan (yasirovic2009@gmail.com)
[2]Universiti Teknologi PETRONAS, Seri Iskandar, Perak, Malaysia

Abstract

This paper investigates the impact of thermal stress on the development of coal fractures. The samples were taken from Balingian Province which represents highly volatile bituminous coal. SEM micrographs of coal showed fracture patterns that look like desiccation cracks. In almost all literature on coal, studies of coal fractures showed interest in fracture impact on coal properties, and the origin of such fractures offered less interest. Coal samples were air dried by evacuation and heated for different temperature ranges to investigate the thermo-mechanical behavior of such coals. Different petrographic and chemical characterization methods were used in coal characterization including thin sections, SEM, elemental mapping aided with EDX and FTIR methods. Besides the development of existing fractures, new fractures developed, the developed fractures proved to directly correlate to temperature applied. The results obtained showed a good link between coal petrography and coal thermal history. The study can be significant for improving the coal permeability through the artificial creation of new fractures and cleats using thermal methods.

Introduction

Coal is known to power almost 40% of Earth's current electricity production. Coal is an important material because not only it is the main source of fossil energy, but also, it is considered as one source of CO_2 that leads to global warming. Recently, in the late 90s, coal gained an increasing interest because of the introduction of technologies to extract coalbed methane (CBM). CBM refers to the gas, which is normally methane that is adsorbed into the solid matrix of coal.

Presence of fractures in coalbeds is one of the factors that increase the permeability of coalbeds. Fractures normally occur as a result of many factors; these include coal matrix shrinkage resulting from the reduction of free surface energy (Murray, 1996). Fractures are also induced by folding processes and are considered to enhance the coalbed permeability (Warwick, 2005). Coal is also characterized by mechanical fractures

that result from explosive materials applied upon coal mining (Everett, 1985), as well as those related to open hole completion geomechanics (Murray, 1996; Michel and Fournier, 2008).

A famous type of fractures that abruptly terminates against underlying strata is known as cleat (Close, 1993). The origin of cleats is not well understood, however, Gayer (1993) suggests that the development of such cleats in coal is associated with dewatering during coal material compaction. Cleats are described as natural fractures that enhance gas flow and facilitates coal reservoir mining (Warwick, 2005).

Desiccation fissures are a kind of fracture that occur in the raw material of coals such as wood trunks, and normally characterize the coal with a blocky appearance (Diessel, 1992).

In many sources it is shown that the increase of volume/porosity of coal fractures is found to be influenced by gas release or desorption and drop in pressure (Harpalani and Chen, 2005). A relationship between coal swelling and coal fractures was observed. In such kind of fractures, referred to as spontaneous fractures, chemical agents such as ammonia was used to induce the swelling of coal and consequently, fractures (Keller and Clay, 1976). It is therefore assumed that these fractures are formed in situ as a result of desiccation. The main objective of this paper was to test the impact of thermal stress on the development of coal samples.

Materials and Methods

Balingian Province is located to the southwest offshore Sarawak area which is tectonic bordering to the Mukah Province. It is characterized by a complex fault system characterized by the West Balingian Line, across which there is a very sharp contrast of tectonic style into the Balingian Province (Hutchison, 1992). The Balingian Formation (sometimes known as Tatau Formation) unconformably underlies the Begrih Formation (Figure 1) along the Mukah Road. It consists of a thick, exceeding 3500 m, sequence of sandstone, pebbly sandstone, fossiliferous mudstone, abundant coal and lignite with seat earths of rootlet mudstone (De Silva, 1986). The Balingian coal area occupies the coastal plain between the Mukah and the Balingian River (Wolfenden, 1960). The Bintulu coal deposit occurs in Miocene paralic strata (Kho, 1966). The coal of the Balingian is estimated at 2 Mt of bituminous coal considered as mineable, but less than half will be accessible by open pit. According to Ni and Abdullah (2004), the Mukah-Balingian coals show a low rank of coalification ranging from Lignite to Sub-bituminous coals based on vitrinite reflectance that ranges between 0.34-0.54 % Ro.

The coals of Mukah-Balingian are considered early thermogenic stage based on the vitrinite reflectance of the exposed Mukah-Balingian coal which ranges from 0.34%-0.54% (Ni and Abdullah, 2004). The Balingian coal was characterized from different prospects including its caloric value. The results showed that the Balingian coal is highly volatile, with volatile matter around 40 %, fixed carbon of around 40 % as well, 15% moisture content, and 6-8 % as ash (Othman and Bosrooh, 2007).

Data on coal pyrolysis can be found and interpreted from the same previous source. Pyrolysis of the same coal samples showed that pyrolysis of the coal can be clearly categorized into three zones: Zone I represents the evolution of water and occurs below 200 °C. Zone II falls within temperature range 200-600 °C. Compounds containing carbon, hydrogen, and oxygen are released as the result of reactions of the functional

groups. This is termed the primary devolatilization range. Zone III contains the second decomposition range (600-900 °C) in which mostly methane and hydrogen are evolved.

Samples were first air dried using vacuum chamber before heating at different temperatures. Samples were then heated in a furnace oven for overnight at 50 °C.

The petrographic characterization was based on Scanning Electron Microscopy (SEM) which provides a good 3D topographic surface map and allowed the visualization of coal surface features as well as associated minerals. The SEM equipment (brand Zeis) is attached with energy dispersive X-ray analytical tool (EDS) that allowed both point elemental analysis and elemental mapping. Elemental mapping was helpful in the study of the distribution of the constituents.

Total organic carbon (TOC) determination was done using solid TOC analyzer of the brand HT 1300 by Analytikjena. The equipment was using a constant temperature range of 800 °C. Powdered samples were heated in the heating chamber to the specified temperature until the combustion curve declined from the peak to the zero-point indicating the total loss of carbon from the samples. Results were obtained using the associated software package.

Results

Generally, coal composition is characterized by some major elements that are present in varying amounts including oxygen, hydrogen, nitrogen, and sulfur, besides some other trace elements (van Krevelen, 1961; Gluskoter, 1975; Speight, 1994); Elemental analysis from EXD showed that the coal samples are composed of dominantly 70% oxygen, with the remaining fraction composed of iron, sulfur, silicon, aluminum, calcium, and potassium. The elements silicon, aluminum, potassium, and iron are most likely reflecting content of some clay. Sulfur is a common mineral associated with coal seams as it reflects formation in a reduced depositional environment. Sulfur in coal can be present in different forms including sulfate minerals, pyrite, and organic sulfur. Iron can be present in coal only from the presence of clay minerals present in the system (Casagrande, 1986). Source of iron in coal other than pyrite is from iron oxides resulting from the oxidation of pyrite (Speight, 2005). Different forms of sulfur present in coal including pyritic sulfur, sulphate, and organic sulfur (Casagrande and Siefert, 1977; Altschuler et al., 1983; Given and Miller, 1985). The elemental composition of the coal samples is shown in Figure 2.

The distribution of such elements can be shown by elemental mapping (Figure 3). The electron mapping shows that oxygen is distributed all over the sample whereas, sulfur is slightly concentrated at the fracture surface.

Chemical characterization of the coal samples using Fourier Transform Infrared is shown in Figure 4. The peaks assigned for different bonds are also shown in Figure 4. The peak at 600 cm-1 was assigned to the stretching vibrations from the linkage between carbon and sulfur (Figure 4). This link can reflect that the sulfur in the coal samples is of organic origin. The peak at 3333 cm-1 can be assigned for three functional groups, which are C-H, OH, and N-H based on the broadness of the peak. The peak for C-H is narrower than both OH and NH, therefore, and based on that the peak is so broad, the peak was assigned for NH group.

Total organic carbon (TOC) was computed for the sample using powdered sample. The total carbon for the sample was estimated at 88 %. As shown in Table 1. The rate for total combustion is shown in Figure 5.

Based on thin sections prepared for the coal samples, the coal samples show high content of vitrinite (indicated by red orange color), with some samples showing Inertinite (identified by dark brown color). Inertinite is minor in abundance and shows granular habits (Figure 6). Pores are shown in white color and they are created during the thin sectioning process.

Original Fracture

The original fracture patterns that inspired this study are characterized by mud-crack-like or desiccation like patterns. The width of such fractures ranges from 1-3 microns, with fracture depth of 4 microns indicating that these fractures are only superficial in nature. The fractures show almost perpendicular intersection that forms small blocks similar to coal cleats. Fracture patterns are shown in Figure 7.

Induced Fractures

Development of coal fractures are shown in Figure 8. Original sample showed fractured width of 3 microns as mentioned earlier (Figure 8A). At 50 °C, fractures show a width of fracture up to 50 microns (Figure 8B). When heated at 100 °C, fracture of 70 microns width are shown (Figure 8C). At the maximum temperature of 150 °C, fracture size approaches 100 microns (Figure 8D).

Discussion

Based on the classification of Neavel (1981) for coal rank, the Balingian coal could be classified as typical bituminous coal (carbon content is 83%). Thin sections of coal do not reflect any form of weathering; therefore, the fracture sets present in the coal cannot be due to weathering. The blocky appearance of the fractures gives the impression these fractures are inherited from the desiccation of the original material. However, the small size (microns) of such fractures cannot be correlated to the large-scale size of desiccation fissures; moreover, transition from raw material to the current coal rank implies many physical, chemical, and bacterial transformations make it impossible to preserve such structures.

Observation of the SEM micrograph of the thermally stressed samples showed the fractures increase with the increase of temperature. It was not possible to trace the same fracture under different temperature ranges. To overcome this problem, SEM captured for the maximum fracture size; and therefore, SEM images presented represent the maximum size of fractures in each temperature range.

Based on the rank of the coal and the amount of moisture content (15%) in literature, the coal is expected to response to thermal stress where it still has some moisture to lose. Therefore, a similar behavior of the original coal is expected in terms of desiccation structures.

It is clear that the relationship between fracture development and thermal stress is direct. The number of samples can allow only showing the response and cannot allow statistical processing of the data to come up with a model. However, a plot between temperature and average width of fractures can display the trend mentioned above (Figure 9).

Conclusion and Recommendations

The Balingian coal showed superficial fracture pattern of 3 microns depth that looks like desiccation cracks and proposes origination from coal dewatering. For testing this hypothesis, heating of dried coal samples under graded temperature ranges showed these fracture sets can develop gradually under thermal stress. Development of such fracture patterns can show the coal properties can be artificially enhanced by applying controlled thermal stress.

References Cited

Altschuler, Z.S., M.M. Shnopfe, C.C. Silber, and F.O. Simon, 1983, Sulfur Diagenesis in Everglades Peat and the Origin of Pyrite in Coal: Science, v. 221, p. 221-227.

Casagrande, D.J., 1986, Sulphur in Peat and Coal, Coal and Coal-Bearing Strata, Recent Advances: Geological Society, London, Special Publications 32, p. 87-105.

Casagrande, D.J., and K. Siefert, 1977, Origins of Sulfur in Coal: Importance of Ester-Sulfate Content: Science, v. 195, p. 675-676.

Chen, K.C., S. Irawan, C.W. Sum, and S.Q. Tunio, 2011, Preliminary Study on Gas Storage Capacity and Gas-in-Place for CBM Potential in Balingian Coalfield, Sarawak Malaysia: International Journal of Applied Science and Technology, v. 1/2, p. 82-94.

Close, J.C., 1993, Natural Fractures in Coal, in B.E. Law and D.D. Rice (eds.), Hydrocarbons from Coal: American Association of Petroleum Geologists, Studies in Geology, v. 38, p. 119-132.

De Silva, S., 1986, Geology of South Mukah-Balingian, Sarawak: B.Sc. Thesis, University of Malaya, Kuala Lumpur, Malaya, 134 p.

Diessel, C.F.K., 1992, Coal-Bearing Depositional Systems: Springer-Verlag, Berlin Heidelberg New York, 727 p.

Everett, L.G., 1985, Groundwater Monitoring Handbook for Coal and Oil Shale Development: Elsevier, Amsterdam-Oxford-New York-Tokyo, 327 p.

Gayer, R.A., 1993, The Effect of Fluid Over-Pressuring on Deformation, Mineralization and Gas Migration in Coal-Bearing Strata, *in* J. Parnell, A.H. Ruffell, and N.R. Moles (eds.), Contributions to an International Conference on Fluid Evolution, Migration and Interaction in Rocks: Geofluids 1993 Extended Abstracts, Torquay, p. 186-189.

George, J.D., and M.A. Barakat, 2001, The Change in Effective Stress Associated with Shrinkage from Gas Desorption in Coal: International Journal of Coal Geology, v. 45/2, p. 105-113.

Given, P.H., and R.N. Miller, 1985, Distribution of Forms of Sulfur in Peats from Saline Environments in the Florida Everglades: International Journal of Coal Geology, v. 5, p. 397-409.

Gluskoter, H.J., 1975, In Trace Elements in Fuel, in S.P. Babu (ed.), Advances in Chemistry Series 141: American Chemical Society, Washington, DC, p. 1-22.

Gray, D., G. Barrass, J. Jezko, and J.R. Kershaw, 1981, Coal Structure and Coal Science: Overview and Recommendations: Coal Structure, American Geochemical Society, Washington DC, 370 p.

Harpalani, S., and G. Chen, 2005, Estimation of Changes in Fracture Porosity of Coal with Gas Emission: Fuel, v. 74/10, p. 1491-1498.

Hutchison, C.S., 1992, Geology of Northwest Borneo: Sarawak, Brunei, and Sabah: Elsevier Publishing Company, 404 p.

Keller, D.V., and C.D. Smith, 1976, Spontaneous Fracture of Coal: Fuel, v. 55/4, p. 273-280.

Kho, C.H., 1966, The Bintulu Coalfield: Prospecting Results: Annual Report for 1965, Geological Survey, Borneo Region, Malaysia, p. 40-68.

Michel, T., and H. Fournier (eds.), 2008, Coal Geology Research Progress: Nova Science Publishers, New York, 255 p.

Murray, D.K., 1996, Coalbed Methane in the USA: Analogues for Worldwide Development, Coalbed Methane and Coal Geology: *in* R. Gayer and I. Harris (eds.), Geological Society, London, Special Publications 109, p. 1-12.

Neavel, R.C., 1981, Origin, Petrography, and Classification of Coal, *in* M.A. Elliott (ed.), Chemistry of Coal Utilization: 2nd ed., Wiley, NY, p. 91-158.

Ni, C.C., and W.H. Abdullah, 2004, Coal Depositional Settings of Mukah-Balingian, Sarawak: Implications for Coaly Petroleum Source Rocks of the Balingian Province: Petroleum Geology Conference and Exhibition 2004, 15-16 December 2004, Istana Hotel, Kuala Lumpur, Malaysia.

Othman, N.F., and M.H. Bosrooh, 2007, Pyrolysis of Sarawak Coals Merit Pila and Mukah Balingian: Jurnal Mekanikal, v. 24, p. 47-55.

Speight, J.G., 1994, The Chemistry and Technology of Coal: 2nd ed., Marcel Dekker, New York, 528 p.

Speight, J.G., 2005, Handbook of Coal Analysis: John Wiley & Sons, 238 p.

Van Krevelen, D.W., 1961, Coal: Elsevier, Amsterdam. 514 p.

Warwick, P.D., 2005, Coal Systems Analysis: A New Approach to the Understanding of Coal Formation, Coal Quality and Environmental Considerations, and Coal as a Source Rock for Hydrocarbons: The Geological Society of America Special Papers, v 387, 118 p.

Wolfenden, E.B., 1960. The Geology and Mineral Resources of the Lower Rajang Valley and Adjoining Areas, Sarawak: Geological Survey of British Borneo, Memoir 11, 167 p.

Zin, I.C.M., 2000, Stratigraphic Position of the Rangsi Conglomerate in Sarawak: Proceedings Annual Geological Conference 2000, Geological Society of Malaysia, p. 131-136.

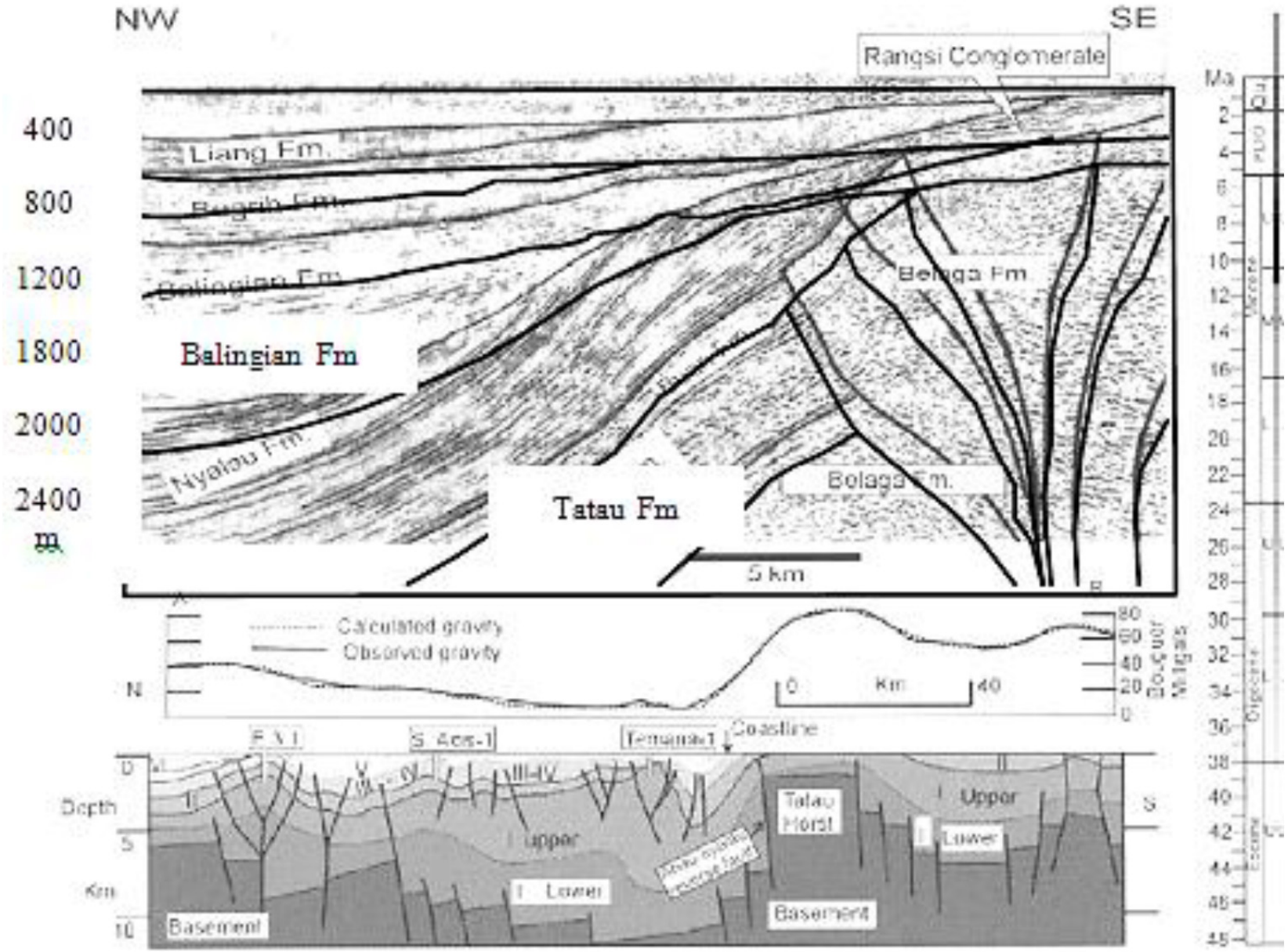

Figure 1. Seismic section showing the stratigraphic position of the Balingian Formation (After Zin, 2000).

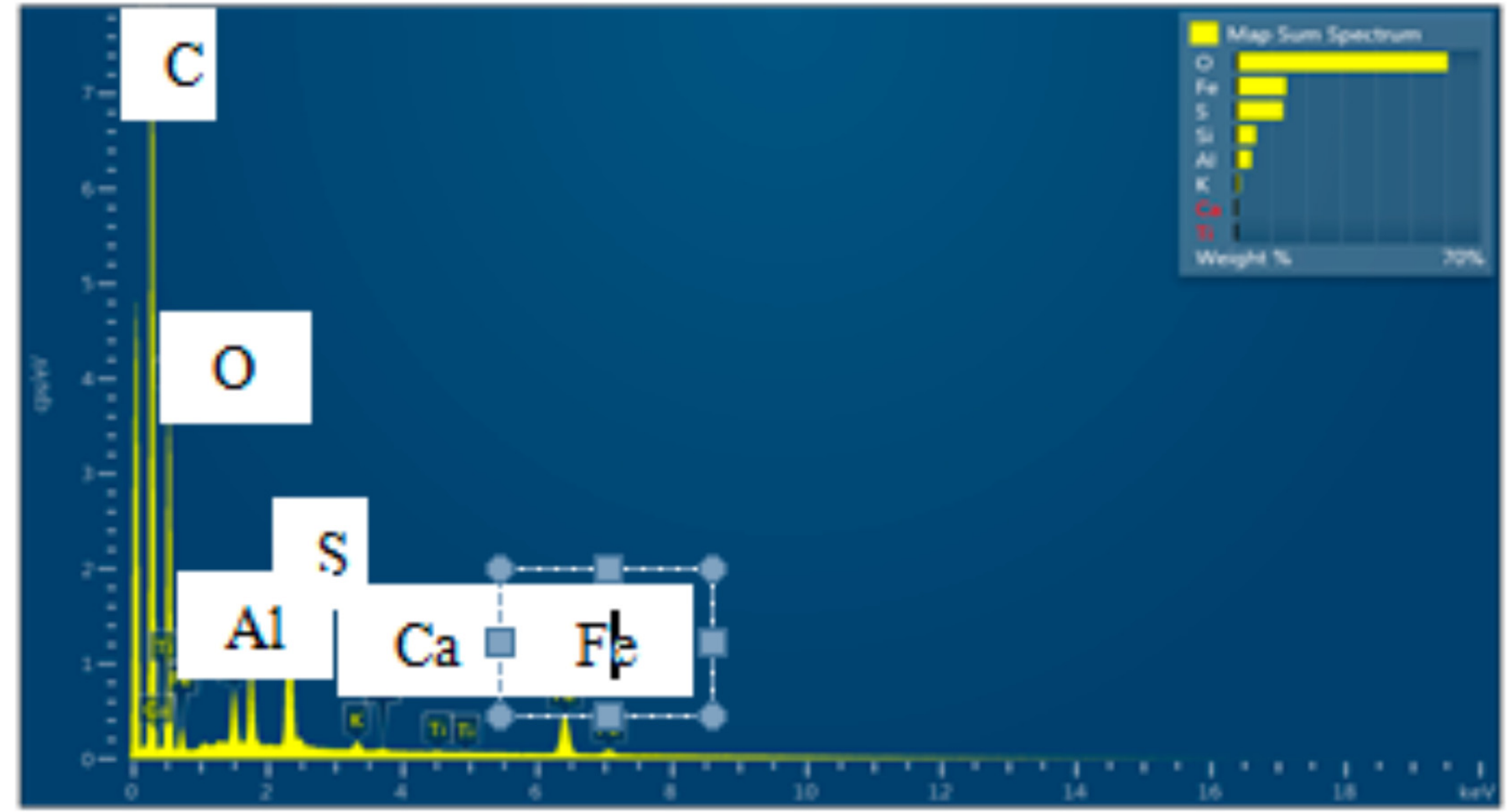

Figure 2. EDX spectrum with elements dominancy represented by the number of counts per second (cps).

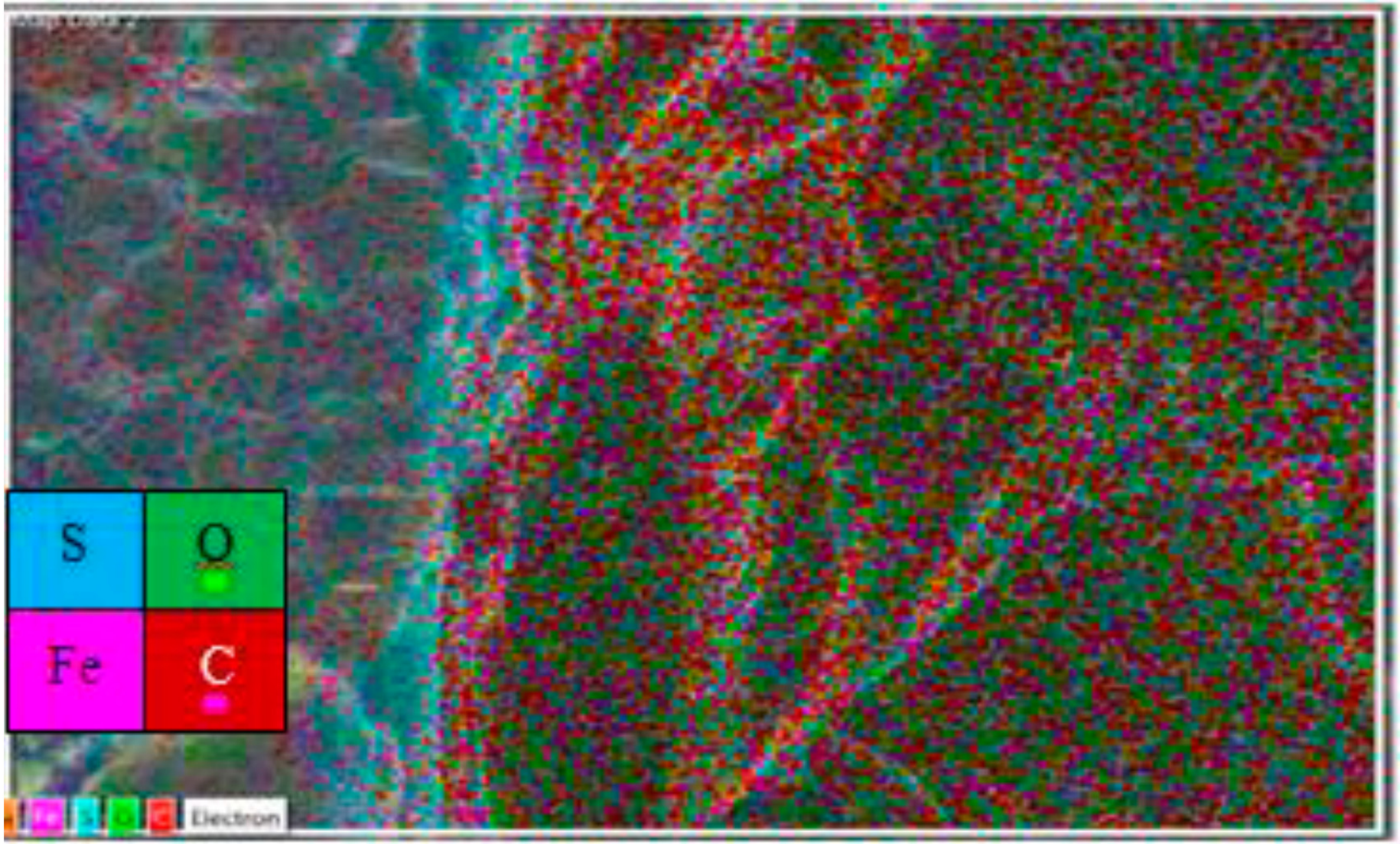

Figure 3. Elemental mapping of the elements present in the coal sample (S2).

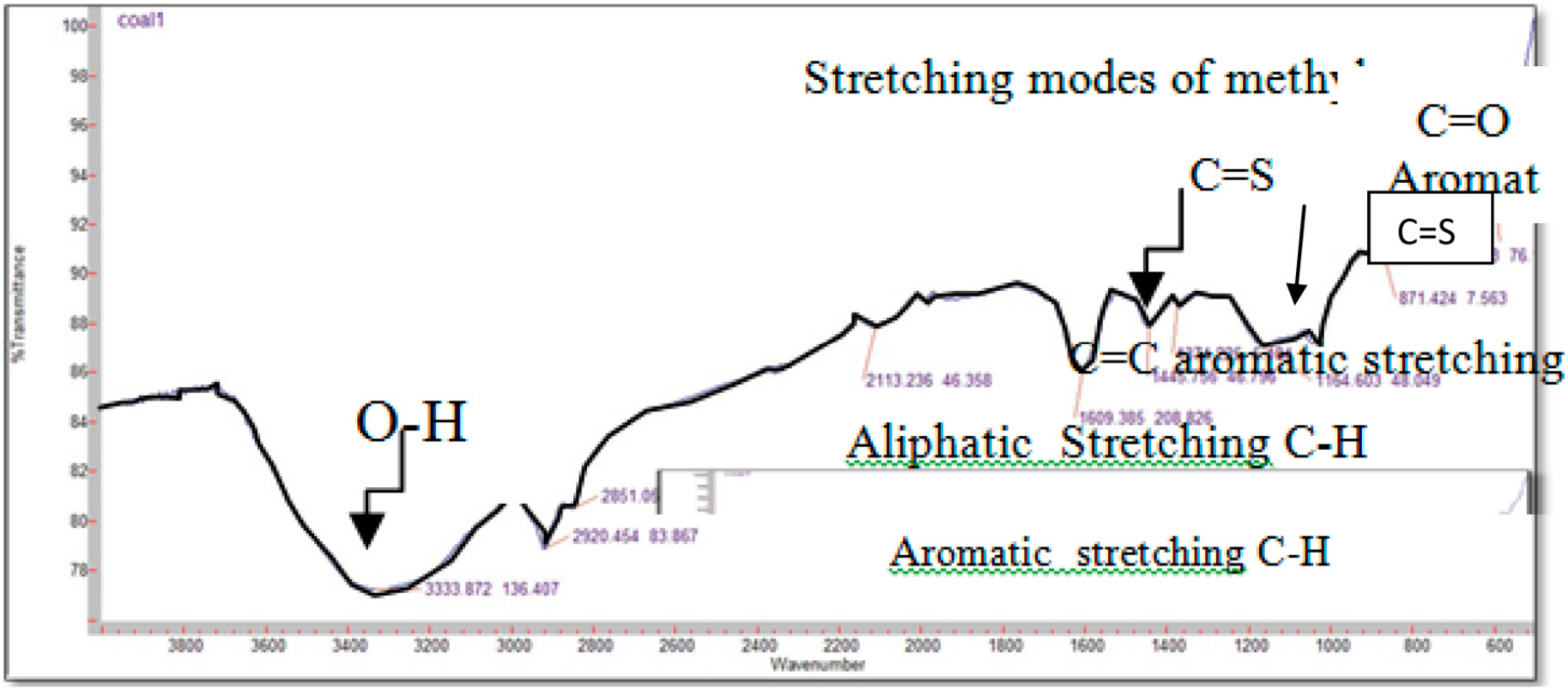

Figure 4. FTIR spectrum of coal sample 1 showing different functional groups present in coal.

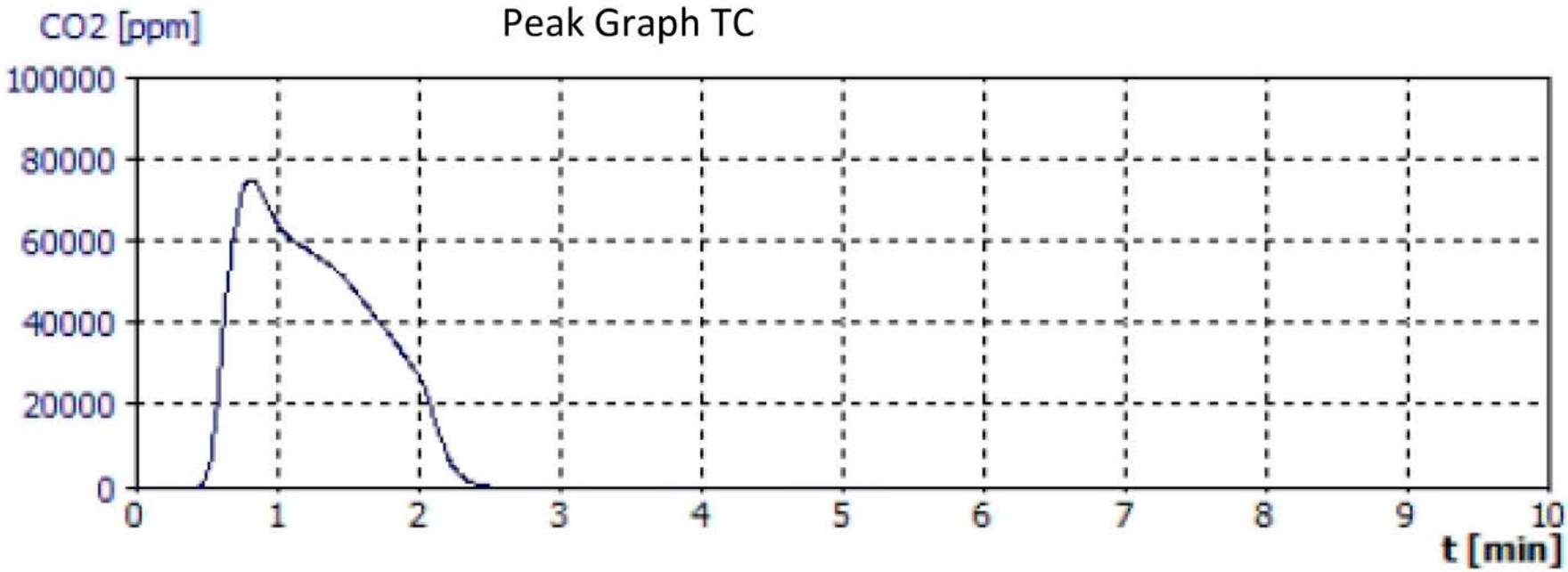

Figure 5. TOC Combustion curve for coal sample 1 showing peak graph.

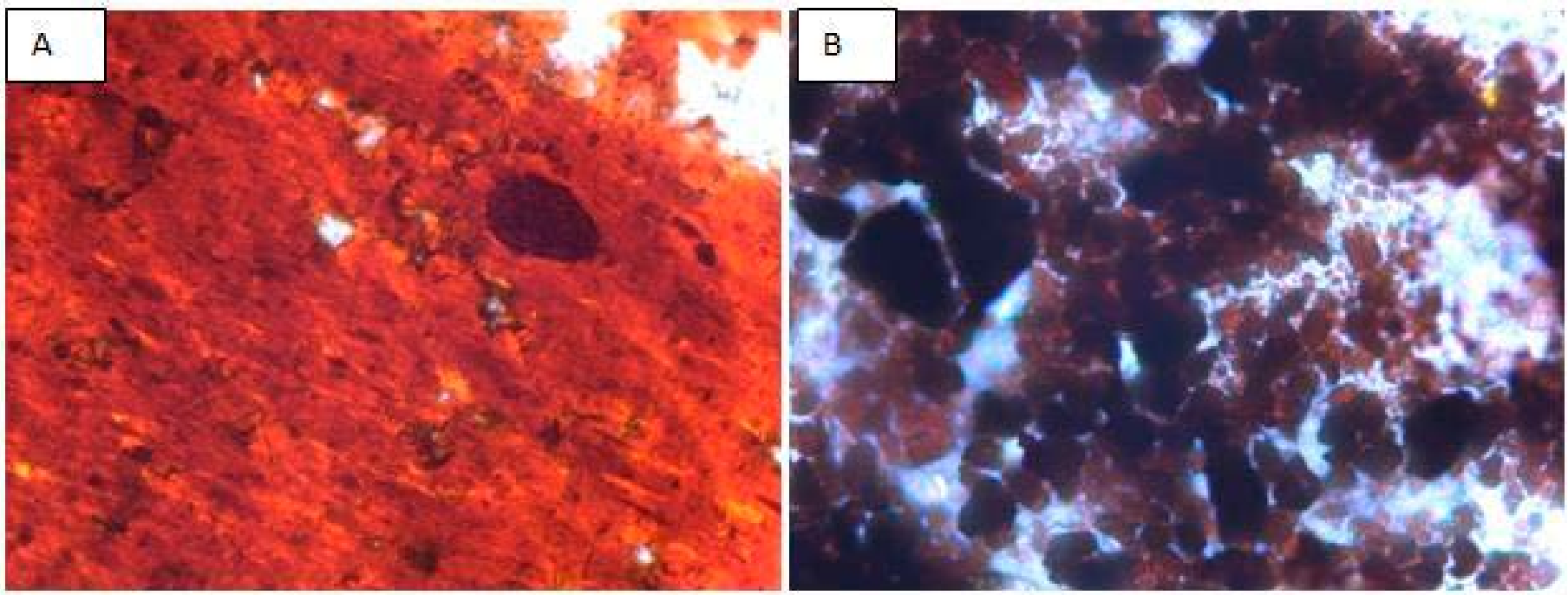

Figure 6. Thin sections of coal: A: Thin section of coal showing dominancy of vitrinite (red orange color), and minor granular inertinite (Sample 1). B: In Sample 2, besides vitrinite, granular inertinite is disseminated (dark brown color). White color reflects pores created during thin sectioning. Thin section magnifications are 40 and 100 times respectively.

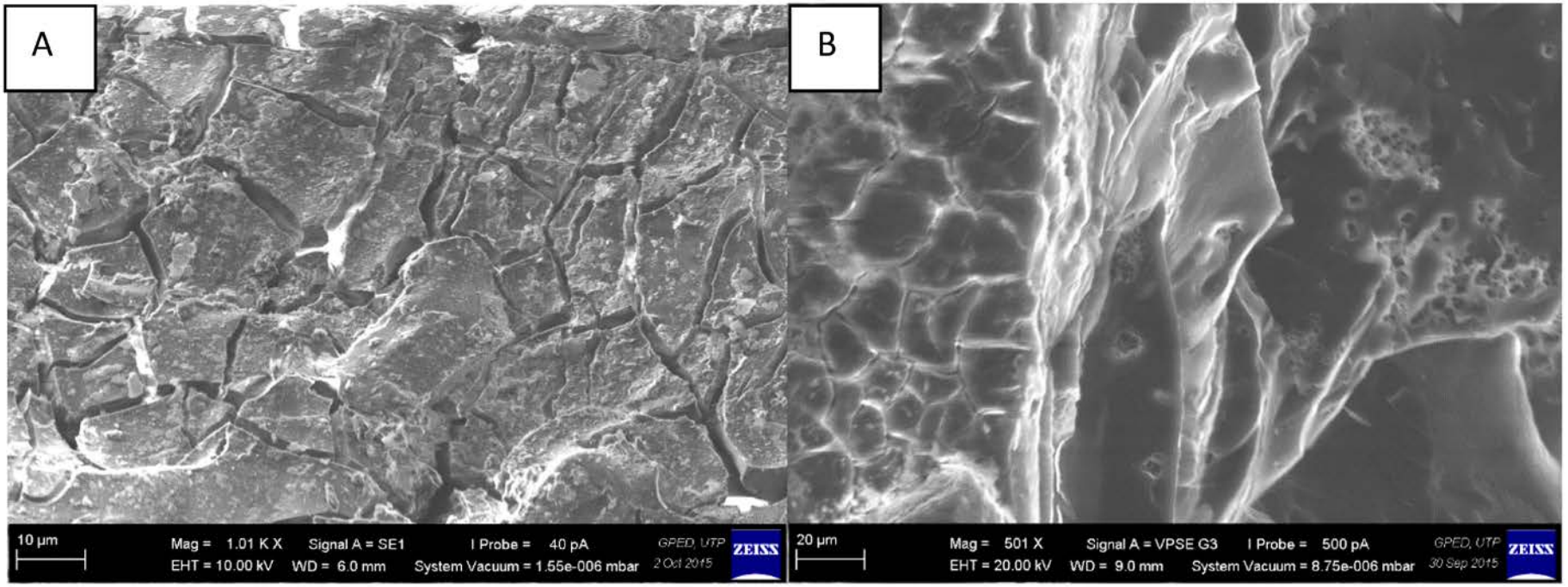

Figure 7. Original fractures: A: Desiccation-crack-like pattern. B: Side view of coal shows that coal fractures are only superficial.

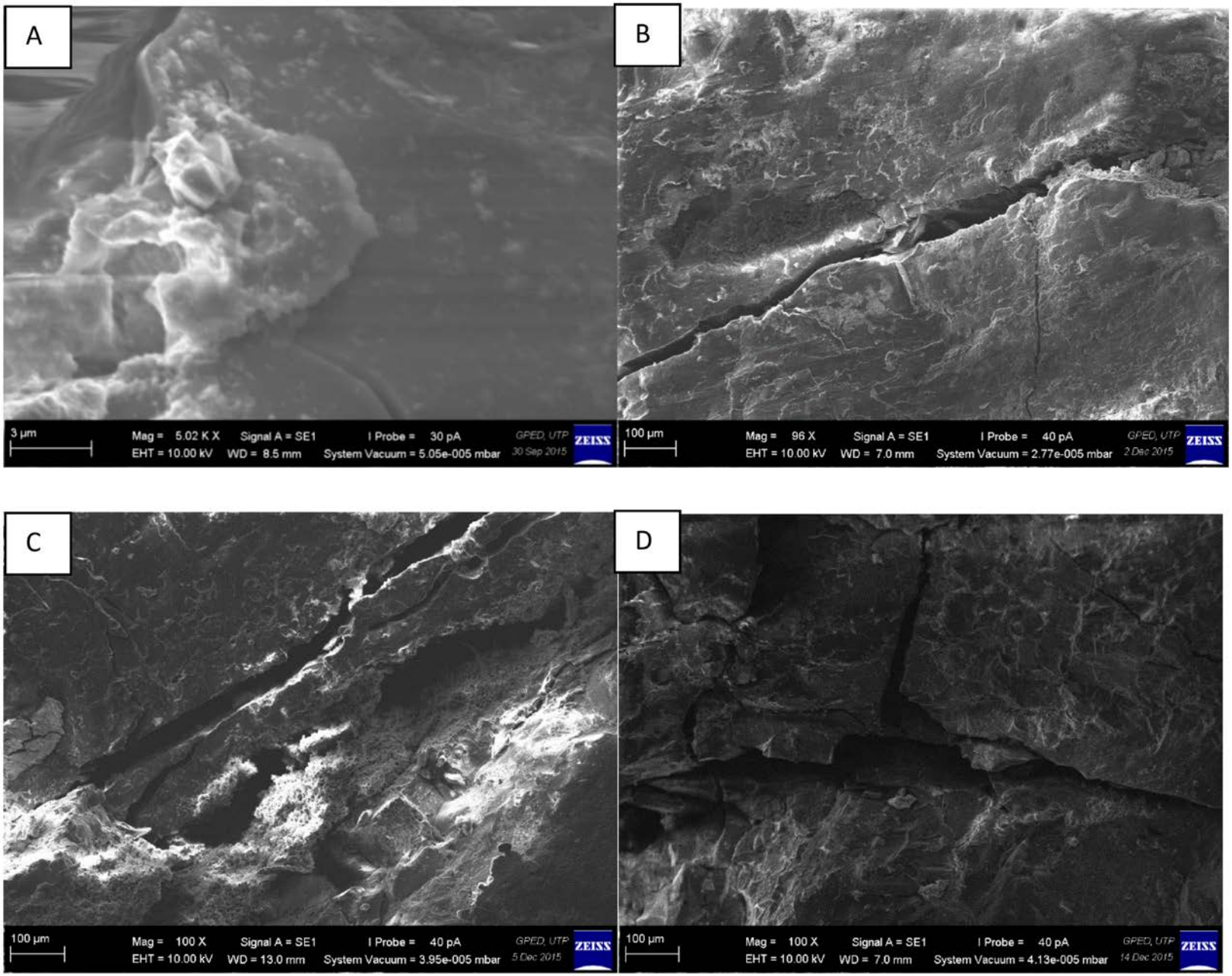

Figure 8. Fracture development at different temperature ranges: A: Original sample. B: B, C, and D: fracture sets at 50, 100, 150 °C.

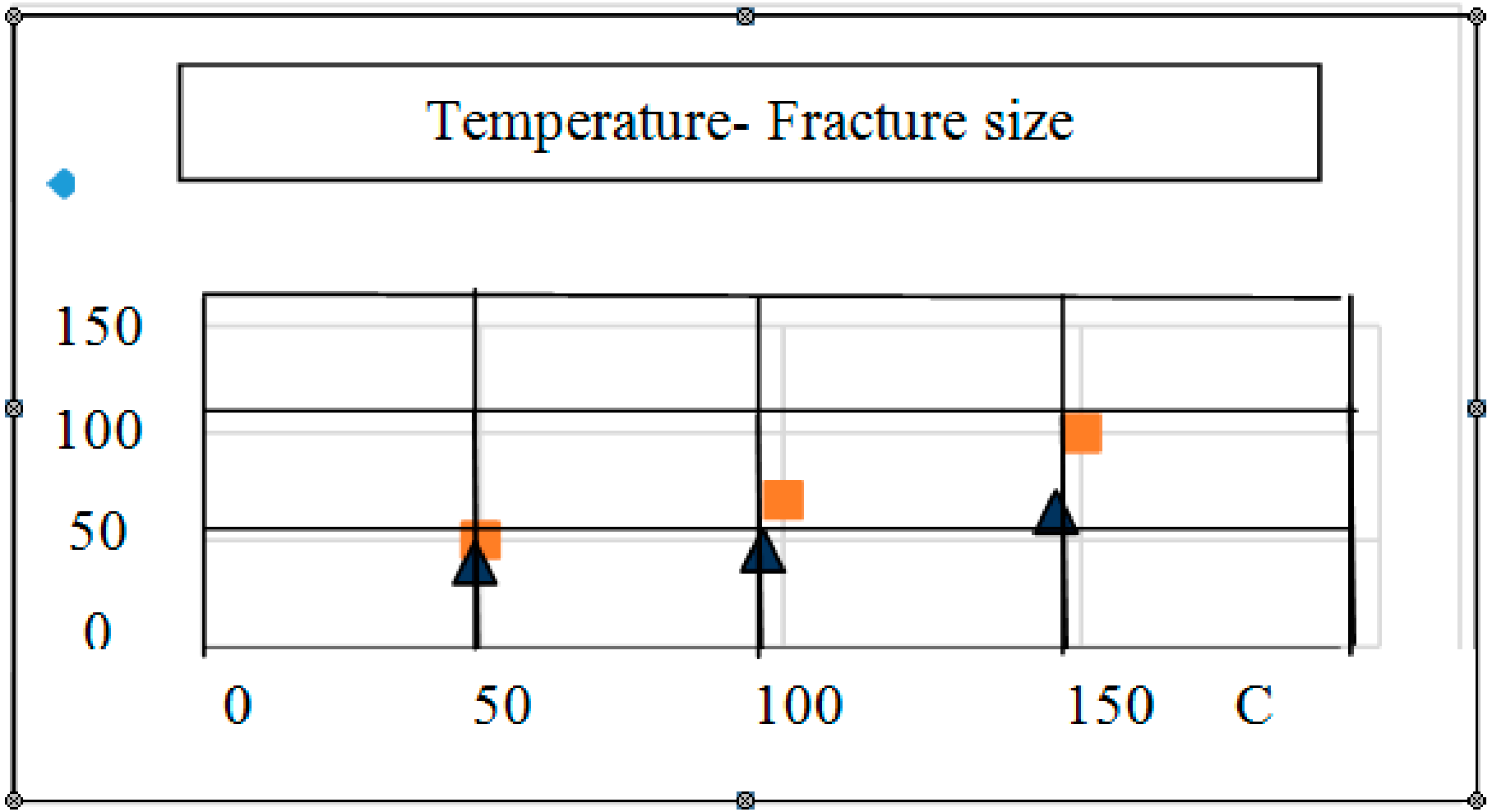

Figure 9. A plot showing the relationship between thermal conductivity and average fracture width.

	C	Ieff	SD	ev	K0	kI	K2	DF
TC	88.3%	1.01E7AU			-6.6102	8.7E-3		1

Table 1. Total carbon for the sample (C). Other values represent coefficients of the combustion reaction.